The relationship between chemical microstructure, crystallinity, mechanical properties, and CO2 / N2 gases permselectivity of thermoplastic polyurethane membranes

Reza Abedi
Department of Chemical Engineering, Ahar Branch, Islamic Azad University
Behnaz MemarMaher (be.maher@iau.ac.ir)
Department of Chemical Engineering, Ahar Branch, Islamic Azad University
Leila Amirkhani
Department of Chemical Engineering, Ahar Branch, Islamic Azad University
Mostafa Rezaei
Institute of Polymeric Materials, Polymer Engineering Department, Sahand University of Technology
Sona Jamshidi
Department of Chemical Engineering, Tabriz Branch, Islamic Azad University

Research Article

Keywords: Thermoplastic Polyurethane (TPU), Membrane, Permselectivity, Mechanical properties, Polycaprolactone, Crystallinity

Posted Date: June 15th, 2023

DOI: https://doi.org/10.21203/rs.3.rs-3019786/v1

Additional Declarations: No competing interests reported.

Abstract

In this study, thermoplastic polyurethane (TPU) with 30%wt hard segment content (HSC) was synthesized using isophorone diisocyanate (IPDI), 1, 4-butanediol (BDO) as the chain extender, and polycaprolactone (PCL) with three different molecular weights (2000, 4000, and 10000) as polyols. Fourier-transform infrared spectroscopy (FTIR), hydrogen nuclear magnetic resonance (H-NMR), X-ray diffraction (XRD), and differential scanning calorimetry (DSC) analysis were used to evaluate the chemical microstructure and physical characteristics of polycaprolactones (PCLs) and thermoplastic polyurethanes (TPUs). The results showed that the crystallinity and the glass transition temperature (Tg) of TPUs became different depending on the molecular weight of the PCL soft segments. A tensile strength was used to evaluate the mechanical properties of TPUs. It was observed that increasing the molecular weight of PCL decreased the elongation at break and increased the ultimate tensile strength. The permeability of CO_2 and N_2 gase over wide ranges of pressure (3 to 9 atm) was examined, and the permselectivity of the membranes was determined. It was concluded that an increase in the feeding gas pressure led to an increase in the gas permeability of all samples. It was observed that in TPU samples, the increase in the molecular weight of PCLs led to a decrement in selectivity and an increase in permeability of CO_2 and N_2 gas.

1. Introduction

Membrane separation technology is one of the current methods of separation technology developed in recent decades. Today, air pollution has been raised as a significant challenge due to harming people's health and the environment. Research with different methods has been tried to remove harmful gases. One of the most common methods for separating gases is the membranes. The efficiency of the membrane depends on its constituents and manufacturing method. Most of the membranes made and used in industries are polymeric [1, 2]. Gas separation is one of the leading industrial applications of membrane technology, which is used in a wide range of air and natural gas dehumidification or removal of organic gases from air streams. Different dense and porous membranes can be used as gas separators [3, 4]. The efficiency of a gas separation membrane depends on the type of material (polymeric or nonpolymeric) [5–9], structure [9–14], and morphology [15, 16, 17]. Most polymers lack properties such as low-temperature flexibility, air absorption, and fatigue resistance and do not perform well in different temperature conditions. However, thermoplastic polyurethane (TPU) has good properties in this field [18–21].

Thermoplastic polyurethanes (TPU) is a class of polymers that are used in membrane applications [22, 23, 24]. Polyurethanes have a microphase-separated structure, which also affects the permeation of gas on it, and gas can diffuse through the phases due to their chemical structure. One of the reasons for using this type of polymer in membrane applications is the presence of these phases [25, 26, 27]. TPUs are the first thermoplastic elastomer material produced by conventional methods which are used for manufacturing thermoplastic polymers [6, 7, 17]. Although these materials have a rubbery behavior, they are processed like thermoplastic [17, 27, 28]. TPU is usually a segmented polymer system in which hard and soft domains are alternately located in the polymer chain. The soft segment, including polyol, gives

elasticity and flexibility to the polymer, and the hard segment which consists of the urethane linkage between diisocyanate and diamine or diol, provides the mechanical strength for the polymer [10, 11, 23, 26]. The performance of the TPU membrane depends on properties such as hydrogen bonding index (HBI), molecular weight, the molar ratio of isocyanate and polyol, the hard segment content (HSC), degree of crystallinity, the orientation of polymer chains, glass transition temperature and the degree of crosslinking. Literature reviews indicate that the increase in gas permeability depends on the type of polyol, and a stronger hydrogen bond [8, 15, 25, 26].

In the synthesis of thermoplastic polyurethane, the stoichiometric ratio (the molar ratio) and ratio of the isocyanate to hydroxyl (NCO/OH) are critical for controlling the synthesis conditions and mechanical properties of the final products. Considering that the participating materials react with each other stoichiometrically with high efficiency, the final polymer structure can be determined by the select molar ratio of -NCO and -OH[6, 7, 17]. The preparation of TPU can be done by two methods, such as pre-polymerization and one-step approaches. In the pre-polymerization method, the prepolymer is obtained from the reaction of a polyol with isocyanate; therefore, the prepolymer has -NCO at the end of the chain, next the prepolymer is reacted with a chain extender to reach the final polymer. This type can be synthesized by melting polymerization and solution polymerization in an appropriate solvent [7, 17, 29].

TPU can be used in membrane preparation for gas separation purposes. The penetration of gas in dense membranes occurs in three stages: the adsorption of gas molecules on the membrane surface, the diffusion of gas molecules through the membrane, and the desorption of gas molecules through the outer surface of the membrane [7, 10, 13]. However, different variables affect permeability, one of them is gas pressure. For example, nitrogen permeability doesn’t change so much with increasing pressure. In contrast, methane permeability decreases with increasing pressure, but the increase in pressure leads to a rise in carbon dioxide permeability. In the case of carbon dioxide permeability in polyurethane, the permeability is higher due to the dissolution of this gas in the polymer [13, 14, 15, 16].In this study, TPU was synthesized by the pre-polymerization method, and its membranes were prepared via the solution casting route. Isophorone diisocyanate (IPDI) as isocyanate, Polycaprolactone (PCL) as a polyol, and 1,4-Butanediol (1,4 BDO) as the chain extender were used. It differs from other studies by changing the reaction time and steps of adding ingredients. PCLs with different molecular weights were synthesized by the ring operation method. To investigate the effects of the PCL soft segment’s molecular weight on TPU final properties, polyurethanes were synthesized with different molecular weights of PCL. However, in all the synthesized samples, the NCO/OH ratio was kept one, by changing the molar ratio of raw materials. XRD patterns were used to evaluate TPU’s crystalline structure. DSC analysis was used to examine their thermal properties. H-NMR was used to study their chemical structure. The tensile test was used to evaluate the mechanical properties, and the CO_2 and N_2 permeation tests were used to assess their gas permeability properties.

The main purpose of this study is to investigate the relationship between the chemical and physical structure of the synthesized polymer and the effect of physical and mechanical properties on gas permeability.

2. Experimental

2.1 Materials

Isophorone diisocyanate (IPDI, M_W: 222.3 g/mol), 1,4-Butanediol (BDO, $C_4H_{10}O_2$, M_W: 90.122 g/mol), ε-caprolactone (CL, $C_6H_{10}O_2$, M_W: 114.14 g/mol), Dibutyltin dilaurate (DBTDL, $C_{32}H_{64}O_4Sn$, M_W: 631.56 g/mol), Tin (II) 2-ethyl hexanoate or stannous octoate (Sn $(Oct)_2$, $C_{16}H_{30}O_4Sn$, M_W: 405.122 g/mol), Dimethylformamide (DMF, Mw: 73.09 g/ mol), Toluene (C_7H_8, M_W: 92.141 g/mol) were purchased from Merck Co., Germany. CO_2 and N_2 gas with a purity of 99.95% mol were supplied by the Barfab Co., Iran.

2.2. PCL synthesis

Polycaprolactone (PCL) was synthesized by the ring-opening polymerization method [29, 30, 31, 32]. As a representative, for the synthesis of 20 g PCL (M_W: 2000 g/mol), toluene (35 ml) as solvent was mixed with stannous octoate as catalyst (0.225 mmol, 0.091g) and BDO as the initiator (9.98 mmol, 0.88 ml), then poured in a three-neck flask at 90°C, mixed for 30 min. After that, ε-caprolactone monomer (0.175 mol, 18.6 ml) was added and mixed at 110°C, for 24 h to complete the reaction. All processes were done under an N_2 atmosphere. To precipitate PCL, methanol at a ratio of 10/1 (V/V) relative to the polymer solution was used and the product was dried at 50°C in a vacuum oven for 24 h. H-NMR analysis was used to determine its molecular weight. The following recipes (Table 1) were used to synthesize PCL with various molecular weights [29].

Table 1
The number of precursors for PCLs synthesis.

Molecular Weight (g/mol)	Toluene (ml)	Stannous octoate (g)	BDO (ml)	ε-caprolactone (ml)
2000	35	0.091	0.88	18.7
4000	35	0.047	0.44	18.7
10000	35	0.0185	0.18	18.7

2.3 TPU synthesis

For the synthesis of TPU with 30%wt hard segment content (HSC), three types of PCLs with molecular weights of 2000, 4000, and 10000 g/mol were used as a polyol, IPDI as diisocyanate, BDO as chain extender, and DBTDL as the catalyst. The NCO/OH ratio in TPUs was kept at one [14, 15, 21]. The pre-polymerization method was used for TPU synthesis. In this method, the desired amount of PCL and DBTDL was mixed with toluene as a solvent with a mass ratio of 1 to 2, and IPDI was added to the mixture in a three-neck flask immersed in an oil bath at a temperature range of 80 to 90°C and stirring speed of 300 rpm for 24h. During the synthesis of prepolymer, IPDI has the lowest chemical reaction rate compared to the other diisocyanates. For this reason, more time must be considered for TPU synthesis [6, 7, 18]. To complete the polymerization process, the desired amount of BDO was added to the solution as

a chain extender. After 4 h,, the resultant polymer was placed in a vacuum oven at 110°C for 48 h. The molar ratio of the precursors is presented in Table 2. The reaction scheme to synthesize TPUs is demonstrated in Fig. 1.

Table 2
The molar ratio of TPU precursors.

Material	TPU 2000	TPU 4000	TPU 10000
IPDI	3.45	6.49	15.15
PCL	1	1	1
BDO	2.45	5.49	14.15
Catalyst: 2.3×10^{-7} mol/cm^3			

2.4 Preparation of TPU membranes

the solution casting method was used to prepare the membrane. In the solution casting method, the polymer solution is poured into a mold, and a membrane is formed after the evaporation of the solvent [18, 19, 20, 21].

Membranes were prepared with a thickness of 150 to 200 µm and a diameter of 8 cm. Procedure to prepare this membrane,1 g of TPU was dissolved in 10 ml of DMF at a temperature range 80 to 90°C under 300 rpm stirring speed for 24 h. The solution was then poured into a Teflon mold and left at room temperature for two days. the reason for this event is to reach temperature stability, removal of small bubbles caused by rapid evaporation of solvents and film uniformity [19, 20, 22]. The membrane was placed in the a vacuum oven with fan at 60°C for 24 h.

2.5 Characterization methods

The chemical structure of synthesized PCLs with various molecular weights (Table 1) and TPUs was characterized via H-NMR spectroscopy. H-NMR analyses were recorded at 25°C with a Bruker 400 MHz spectrometer (Ultra Shield 400, Germany). Chloroform (CDCl3) was used as a solvent, and chemical shifts were evaluated with respect to tetramethyl silane (TMS) as the internal standard.

Spectra of Fourier transform infrared spectroscopy(FTIR) were recorded using a Bruker FTIR spectrometer (Tensor 27, Germany) with a measurement range of 400 to 4000 cm^{-1}. The pellets of PCL samples were recorded in FTIR mode and the film of TPU samples in ATR-FTIR mode.

DSC (Netzsch DSC-200 F3, Germany) method was used for thermal characterization. The samples were analyzed according to the following procedure: first, the samples were heated to 100°C and kept for 3 to 5 min at this temperature to eliminate any thermal history. Then the samples were cooled down to -90°C and held for 3 to 5 min. Finally, they were heated up to 200°C. All thermal stages were conducted under nitrogen purge with a heating and cooling rate of 10°C/min. The degree of crystallinity (Xc (%)) of the

samples was calculated using the heat of fusion of PCL crystals during the second heating stage of the DSC scan relative to the heat of fusion of 100% crystalline PCL (136 J/g) [33, 34].

X-ray diffraction (XRD) patterns of samples were acquired by an X-ray diffractometer (Siemens D5000, Germany) using a copper anode with an accelerating voltage of 35 kV and a current of 20 mA. Samples were scanned in the range 2θ: (10–50) at ambient temperature and at a rate of 0.01 s/step.

To study the mechanical properties of TPU membranes, the Zwick / Roell machine (Z010, Germany) was used. In this analysis, the pre-load value was 0.5 N, and the tensile rate was 10 mm/min according to the ASTM D 638 standard. At least three specimens of each sample were tested.

2.6 Gas permeability measurements

A gas permeation device measured the permeability of CO_2 and N_2 gas. Figure 2 is a schematic of this device. In this device, the permeability test is performed at variable pressures at a constant volume. This measurement was performed at pressures of 3, 5, and 10 atm and ambient temperature. Each experiment was repeated at least three times.

One method for evaluating the membrane performance is to measure pure gas permeates and calculate selectivity. Thus, a circular membrane with a diameter of 2.5 cm is placed in the membrane modulus; pure gas is passed under a certain pressure. A graduated bubble cylinder calculates the volumetric gas flow through the membrane. The samples are exposed to the gas flow for about 0.5- 4h to achieve a steady-state flow (Eq. 1) to calculate the permeability. Giving more time and different filters in the gas path were led to a stable state [18, 19, 20, 21].

$$\mathrm{P}=\frac{\nu\,\mathrm{l}}{\mathrm{A}\times(\,\mathrm{Pfeed}\,-\,\mathrm{Ppermeate}\,)}$$

1

Where "P" according to Barrer (1×10^{-10} cm^3(STP)·cm/cm^2·s·cmHg) indicates the permeability of gas through the membrane, "P_{feed}" (cmHg) is the relative feed pressure, "$P_{permeate}$" (cmHg) is the relative flow pressure, "v" (cm^3/s) is the volumetric flow rate, "A" (cm^2) is the effective membrane surface area, and "l" (cm) is the thickness of the membrane.

Furthermore, the selectivity of CO_2 relative to N_2 is defined as the ratio between the permeability of the two gases [22, 23, 24, 25].

$$\alpha=\frac{\mathrm{P_{CO2}}}{\mathrm{P_{N2}}}$$

2

3. Result & Discussion

3.1 H-NMR analysis of synthesized PCLs

H-NMR analysis is performed to confirm the chemical structure of synthesized PCLs and TPUs. The chemical structures associated with the different protons are shown in Figs. 3 and 4. Intensifications in PCL at δ_A = 1.38–1.42 ppm (-CH_2- CH_2- CH_2-), δ_B = 1.59–1.69 ppm (-CH_2-CH_2-O), δ_C = 2.29–2.32 ppm (-CH_2COO), δ_E = 4.04–4.10 ppm (CH2OCO) appear in repeating groups. The terminal group of PCLs is identified in δ_D = 3.62–3.66 ppm (CH_2OH). The results of the H-NMR spectra showed that PCL was successfully synthesized and followed the proposed structure of Fig. 3 for PCL. Eq. 3 was used to calculate the actual molecular weight of the synthesized PCLs. The results for PCLs are given in Table 3. Note that the peaks appeared in δ = 7-7.3 ppm for $CDCL_3$ as a solvent and in δ = 0.04–0.09 ppm for the TMS marker [29, 33, 34].

Table 3
Calculated the number-average molecular weights of synthesized PCLs.

Sample	A(δ_D)	A(δ_E)	X_{SS}	M_n calculated by H-NMR
PCL 2000	1.00	8.98	17.96	2312
PCL 4000	1.00	18.58	37.16	4503
PCL 10000	1.00	46.23	92.46	10815

$$\mathrm{XSS} = 2\times\frac{\mathrm{A}(\delta\mathrm{D})}{\mathrm{A}(\delta\mathrm{E})}, \mathrm{Mn} = (\mathrm{XSS}\times 114.14)+262$$

3

where "X_{SS}" is the ratio of the areas corresponding to the peaks at the resonances of "δ_D" and "δ_E" and "M_n" is the number average molecular weight of PCL.

For TPUs, the methyl (CH_3) and methylene (CH_2) groups of IPDI and PCL are found in δ = 0.88–1.85 ppm. The methylene and methine groups attached to the nitrogen atom are found in δ = 2.13–3.01 ppm. Methine and methylene groups attached to the urethane oxygen atom were identified at about δ = 4.2–4.6 ppm, respectively [8]. Successful synthesizing of the TPUs was evaluated by the H-NMR spectrum (Fig. 4).

3.2 Hard segment content of synthesized TPUs

As written, in the structure of TPUs, PCL is the soft segment, and the remaining parts of IPDI and BDO are known as the hard segment. Eq. 4 is used to calculate TPU hard segment content [29, 33, 34].

$$\mathrm{HSC}(\%) = \frac{(\mathrm{nIPDI} \times \mathrm{MIPDI}) + (\mathrm{nBDO} \times \mathrm{MBDO})}{(\mathrm{nIPDI} \times \mathrm{MIPDI}) + (\mathrm{nBDO} \times \mathrm{MBDO}) + (\mathrm{nPCL} \times \mathrm{MPCL})}$$

4

Where, "M" is the M_W of the precursors, and "n" is the molar ratio of the precursors. Data in Table 3 was used for M_W of PCLs. Table 4 displays the molar ratio and the weight amount of the precursors. In this study, the hard segment content is fixed for all TPU samples, which leads to changes in the molar ratio and weight amount of the precursor. This means that an increase in M_W for PCL leads to an increase in the molar ratio of precursors. The increase in the number of moles of IPDI and BDO indicates the increase in the molecular weight of the resultant TPU polymer.

Table 4
Hard segment content of TPUs.

Sample	IPDI		PCL		BDO		HSC (%)
	Molar ratio	Mass (g)	Molar ratio	Mass (g)	Molar ratio	Mass (g)	
TPU 2000	3.445	1.665	1	5	2.445	0.480	30
TPU 4000	6.485	1.602	1	5	5.485	0.549	30
TPU 10000	15.150	1.981	1	5	14.150	0.750	30

3.3 FTIR analysis of synthesized PCLs and TPUs

FTIR spectra were used to study the chemical structure of PCLs and TPUs. For PCL samples (Fig. 5), as discussed before, its structure has three important functional groups. The peak at the wave number range (3300–3600 cm^{-1}) corresponds to O-H, and the peaks in the range (2800–3200 cm^{-1}) are related to C-H. A sharp peak in the range (1680–1750 cm^{-1}) is attributed to the carbonyl group (-C = O). Two peaks, one stronger than the other in the wave number range (1100–1300 cm^{-1}), are related to C-O groups.

Three main regions are usually considered to confirm the structure of TPU (Fig. 6) by FTIR spectroscopy. Peaks in the wave numbers (3200–3400 cm^{-1}) belong to the -NH group containing hydrogen bonds and non-bonds. Wave numbers (2800–2950 cm^{-1}) belong to the C-H groups; as well as wave numbers (1680–1730 cm^{-1}) correspond to the free carbonyl groups (C = O) and hydrogen bonded carbonyl groups. The peak corresponds to the free carbonyl group observed at 1700–1730 cm^{-1}, and the peak related to the hydrogen-bonded carbonyl group is observed at 1680–1688 cm^{-1}.

As mentioned, TPUs comprise soft and hard segments and two types of hydrogen bonds between these segments. The hydrogen bonds are conducted between the hard segments (NH and CO of urethane) as well as between the hard and soft segments (NH and CO of ester). The first hydrogen bonding creates phase separation between hard and soft domains, and the second one leads to phase mixing. Using peak

fit software, the area below the free carbonyl and the hydrogen bond carbonyl peaks were deconvoluted. The hydrogen bonding index (HBI) was calculated using the ratio of the area under the peaks and Eq. 5 [29].

$$\mathrm{HBI}\ (\%) = \frac{\mathrm{Ac{=}o\ bonded}}{\mathrm{Ac{=}o\ bonded} + \mathrm{Ac{=}o\ free}} \times 100$$

5

In the structure of TPUs, the urethane carbonyl groups (in the hard segment) and the PCL carbonyl groups (in the soft segment) act as proton acceptor groups, forming hydrogen bonds with the NH groups in the hard segment, which act as proton donors [29, 33, 34].

Table 5 summarizes the HBI for various TPUs. It observed that the increase in the M_W of PCL is the reason for the rise in NH bonding, which leads to an increase in HBI, and finally increase in phase separation between TPU's hard and soft segments.

Table 5
HBI, degree of crystallinity, and crystal size for crystal plates of (110) and (200) in different PCL and TPU samples were calculated by FTIR and XRD experiments.

Sample	$A_{c=o\ bonded}$	$A_{c=o\ free}$	HBI (%)	L_{110} (nm)	L_{200} (nm)	Degree of crystallinity (%)
PCL 2000	N.O. [a]	N.O. [a]	N.O. [a]	27.38 ± 1.78	22.91 ± 1.21	51.85 ± 1.39
PCL 4000	N.O. [a]	N.O. [a]	N.O. [a]	31.50 ± 1.43	24.99 ± 1.01	49.19 ± 1.24
PCL 10000	N.O. [a]	N.O. [a]	N.O. [a]	39.12 ± 1.83	32.91 ± 0.87	42.74 ± 1.17
TPU 2000	5.12 ± 0.46	8.63 ± 0.49	17.55 ± 0.04	N.O. [b]	N.O. [b]	N.O. [b]
TPU 4000	6.32 ± 0.51	8.75 ± 0.45	37.24 ± 0.4	19.55 ± 0.88	17.18 ± 0.56	10.82 ± 1.44
TPU 10000	7.35 ± 0.53	8.83 ± 0.47	45.43 ± 0.05	16.83 ± 1.01	16.25 ± 0.55	20.16 ± 1.66
N.O.[a]: All of them are free carbonyl.						
N.O.[b]: Due to the low crystallinity, no pattern was observed.						

3.5 XRD analysis of samples

The crystalline structure of the samples was investigated using XRD analysis. For PCLs, three index peaks are observed in 2 : (21, 22, 24)°. Which corresponds to the crystal plates 110, 111, and 200, respectively (Fig. 7). These results are consistent with other studies confirming the crystalline structure of PCL [29, 33, 34]. Comparing the patterns of PCL and TPU, some peaks have disappeared. The two significant peaks are observed as the two main reflections in TPUs (Fig. 7). To quantify the effects of PCL molecular weight change in the crystalline structure of the samples, the degree of crystallinity and the size of the crystals in the soft segment of the samples were calculated. Eq. 6 was used to calculate the degree of crystallinity of the samples [33, 34].

$$\mathrm{XC}\,(\%) = \frac{\mathrm{A110} + \mathrm{A111} + \mathrm{A200}}{\mathrm{A110} + \mathrm{A111} + \mathrm{A200} + \mathrm{Aah}} \times 100$$

6

Where, "A_{hkl}" is the area of the crystal plates (hkl) in XRD patterns, and "A_{ah}" corresponds to the amorphous halo.

Figure 7 shows the XRD patterns of the samples. In the TPU2000 sample, no significant XRD pattern is observed due to the very low crystallinity (amorphous) of this polymer sample. Eq. 7 is used to measure 110 and 200 crystal plates size [33, 34].

$$\mathrm{Lhkl} = \frac{\mathrm{K} \times \lambda}{\beta\mathrm{hkl} \times \cos\theta\mathrm{hkl}}$$

7

Where "L_{hkl}" is the size of the crystal plate (hkl), "K" is the Scherer constant (K = 0.9), and "β" is the full-width diffraction at half maximum (FWHM), "λ" and "θ" is the X-ray wavelengths (Equal to 0.01540 nm) and Bragg's angle, respectively [33, 34]. Calculations were performed for all samples. Note that the degree of crystallinity calculated by this method is volumetric and the results may be different from DSC method calculations.

According to the results in Table 5, with increasing molecular weight of PCLs, the degree of crystallinity decreases due to the inhibition of hard segments against crystallization of PCL in TPU chains, especially by means of soft-to-hard hydrogen bonding [29, 33, 34]. But in TPUs, the situation is quite the opposite, so as the polymer chain increases, crystallinity increases due to the increase in phase separation [29, 33, 34]. As previously mentioned, from TPU2000 to TPU10000, the degree of phase separation is increased. The more phase separation, the less prevention imposed by hard segments on soft segments, resulting in a higher degree of crystallinity and increased crystal size.

3.6 DSC analysis

DSC analysis was used to investigate the thermophysical properties of the samples, and the results are given in Table 6 and Fig. 9. As shown in the XRD and FTIR analysis, with increasing HBI, the size of TPUs

crystals is increased. In the DSC analysis, the PCL thermograms show two sharp peaks at temperature ranges of (48–57) ^{o}C and (19–28) ^{o}C corresponding to the melting and crystallization of PCLs. The results (Fig. 10, Table 6) show that the melting temperature is shifted to higher temperatures with increasing PCL molecular weight due to the improved polymer chain crystallinity. Furthermore, TPU thermograms confirm that this polymer's crystalline structure is created from PCL's crystalline structure [29, 33, 34].

Table 6
Degree of crystallinity (X_S), melting point (T_m), glass transition temperature (T_g), and heat of fusion (ΔH_{SS}) of PCLs, and TPUs determined by DSC.

Sample	T_g (^{o}C)	T_m (^{o}C)	ΔH_{SS} (J/g)	X_c (%)
PCL 2000	-58.63 ± 0.61	50.56	82.01	60.30
PCL 4000	-57.12 ± 0.24	55.35	79.13	58.18
PCL 10000	-56.47 ± 0.32	57.98	78.57	57.77
TPU 2000	-37.12 ± 0.45	30.91	0.46	1.58
TPU 4000	-37.31 ± 0.67	34.44	5.63	19.62
TPU 10000	-39.75 ± 0.58	41.91	11.21	31.17

Eqs. 8 and 9 are used to calculate the degree of crystallinity of PCL and TPUs, respectively [32, 34, 35].

$$\mathrm{XS}\,(\%) = \frac{\Delta \mathrm{HSS}}{136} \times 100$$

8

$$\mathrm{XS}\,(\%) = \frac{\Delta \mathrm{HSS}}{\Delta \mathrm{HC} \times (1\text{-}\mathrm{HS})} \times 100$$

9

Where, "ΔH_{SS}" is the soft segment's melting heat (J / g), and "H_S" is the normalized mass of the hard segment.

The DSC results in Tabl 6 confirm the XRD calculations. It should be noted that, unlike the XRD test, in this test, the degree of crystallinity is calculated in terms of sample mass with differences in density. Therefore, there is no need for two values to be equal for different samples. Instead, they should have the same trend.

According to the results of Table 6, it is observed that the increase in the molecular weight of the soft segment (PCL) leads to decreasing the glass transition temperature (T_g) of TPUs. By increasing the crystallinity of TPUs, the mobility of the polymer chain is decreased, which leads to a decrement in the T_g of TPUs.

3.7. Mechanical Properties

A tensile test was performed to evaluate the mechanical behavior of TPU membrane samples. As shown in Fig. 10 and Table 7, as the molecular weight of PCL increases, the tensile strain decreases, and the tensile strength increases. Young's modulus of TPUs is given in Table 3. It is observed that this modulus increases with the increasing molecular weight of PCL. As was previously mentioned, increasing the molecular weight of PCL increases HBI, as well as the crystallinity of the soft segments. The most important factor in the mechanical properties of TPUs is HBI. Due to the increase in hydrogen bonding between the PU chains, an increase in tensile strength is observed. With increasing HBI, the phase separation between hard and soft segments is conducted and the hydrogen bonds only occur between the hard domains, leading to an increment in Young’s modulus. However, in this study, the HSC was kept constant by changing the molar ratio of precursors. It is found that the mechanical properties of the TPU membrane are improved by increasing the molecular weight of PCL [7, 17, 33, 34].

Table 7
Young's modulus, Elongation at the break and yield stress of TPU membranes.

Sample	Young's modulus (MPa)	Elongation at break (%)	Tensile strength (MPa)	Yield strain (%)	Yield stress (MPa)
TPU 2000	24.47	512.86	2.54	5.51	0.77
TPU 4000	496.68	449.65	15.49	3.26	6.82
TPU 10000	661.50	325.61	26.09	6.33	10.50

3.8. Gas permeation properties

The permeability of the membranes at a temperature of 25 ^oC and pressures of 3, 6, and 9 bar for CO_2 and N_2 gas were measured independently. In Fig. 11, the permeability of the gas through the membrane can be seen. It is observed that the permeation of CO_2 is higher than N_2 in all membranes. As mentioned in the introduction, the gas permeation mechanism occurs in three stages: the adsorption of gas molecules, the diffusion of gas molecules, and the desorption of gas molecules through the outer surface of the membrane. The permeation content of gas such as CO_2 through the polymeric membrane relates to its dissolution behavior in polymers. In the polymer structure, the presence of carbonyl groups causes further dissolution of CO_2 gas in the TPU membrane. It is observed that with increasing PCL molecular

weight, this dissolution and, consequently permeability is increased. CO_2 is a weak electrophile that tends to receive electrons. Increased molecular weight and consequently hydrogen bonding in TPUs can be determining factors in increasing CO_2 dissolution in TPU membranes [7, 10, 13].

The permeability and selectivity of gas are given in Tables 8 and 9. For TPU2000, it is observed that it has less permeability for both gas. Less phase separation, low polymer chain mobility, and low HBI have resulted in less gas permeability. However, the selectivity of CO_2 gas is higher than N_2. At a certain pressure, increasing the polymer chain lengths (due to the increase in the molecular weight of PCLs) has improved the gas permeability but reduced the selectivity[4, 16, 24, 25, 26].

Table 8
Permeability of TPU samples.

Permeability (Barrer)				
Gas	Sample	Pressure(atm)		
		3	6	9
CO_2	TPU 2000	7.33	8.12	9.54
	TPU 4000	34.97	67.64	81.28
	TPU 10000	101.50	181.26	302.48
N_2	TPU 2000	0.01	0.02	0.03
	TPU 4000	2.56	6.35	10.76
	TPU 10000	9.86	17.93	42.24

Table 9
Selectivity of TPU samples.

Selectivity(α_{CO_2/N_2})			
Sample	Pressure(atm)		
	3	6	9
TPU 2000	45.33	36.36	27.14
TPU 4000	13.65	10.65	7.55
TPU 10000	10.29	10.11	7.16

In addition, Increasing the gas pressure caused enhancement the permeability and decline of the selectivity, due to the improvement of the solubility of N_2 and CO_2 gas in TPU membranes. However, the change in the rate of dissolution of CO_2 in TPU with pressure variations is higher than N_2, due to the

higher affinity of CO_2 to urethane and carbonyl groups of TPU compared to N_2 gas [4, 17, 14, 16, 24, 25, 26].

4. Conclusions

Thermoplastic polyurethanes containing 30%wt. HSCs were synthesized using IPDI as diisocyanate, BDO as the chain extender, and PCL with different molecular weights as a polyol. PCLs by different M_W (2000, 4000, and 10000 g/mol) were adjusted and then used in TPU synthesis. The H-NMR and FTIR spectra showed that PCL and TPU were successfully synthesized. In addition, FTIR spectra were observed that the increasing molecular weight of PCL caused enhancement of the amount of hydrogen bonding index (HBI) in TPU, which led to an increase in phase separation. XRD analysis showed a decrease in the crystallinity of the samples with PCL molecular weight increment, which was also confirmed by the DSC thermograms. The tensile tests revealed that the increase in the MW of the PCL soft segments and the increase in the HBI of TPU led to an increase in tensile strength and Young's modulus of TPU samples. In the gas permeability test, at all pressures, the increased permeability of CO_2 and N_2 gas was observed with increasing M_W of PCL due to the increased polymer chain length in TPUs. However, due to the saturation of CO_2 in the TPU membrane, the selectivity decreased with increasing molecular weight.

Declarations

All authors confirm that this manuscript has not been published elsewhere and is not under consideration by another journal. All authors have participated in the conception, design, analysis, and interpretation of the data, drafting the article or revising it critically for important intellectual content, and approving the final version. This manuscript has not been submitted to, nor is it under review at, another journal or other publishing venue. The authors have no affiliation with any organization with a direct or indirect financial interest in the subject matter discussed in the manuscript. The authors have no relevant financial or non-financial interests to disclose. The authors declare that no funds, grants, or other support were received during the preparation of this manuscript.

Ethical Approval

This declaration is “not applicable”

Competing interests

The authors declare that they have no known competing financial interests or personal relationships that could have appeared to influence the work reported in this paper.

Authors' contributions

All authors contributed to the design and implementation of the research, to the analysis of the results, and to the writing of the manuscript.

Funding

The authors declare that no funds, grants, or other support were received during the preparation of this manuscript.

Availability of data and materials

All of the data created, procured, or used for this research project can be accessed in this manuscript.

References

1. Das C, Gebru KA (2018) Polymeric Membrane Synthesis, Modification, and Applications: Electro-Spun and Phase Inverted Membranes. Taylor & Francis Group CRC Press, New York, pp 5-11, pp 21-23
2. Khulbe KC (2021) Nanotechnology in Membrane Processes. Springer Nature, Switzerland, pp 23-36
3. Karimi MB, Khanbabaei G, Sadeghi MM (2017) Vegetable oil-based polyurethane membrane for gas separation. J Mem Sci 527:198-206. https://doi.org/10.1016/j.memsci.2016.12.008
4. Joshi M, Adak B, Butola BS (2018) Polyurethane nanocomposite-based gas barrier films, membranes and coatings: A review on synthesis, characterization and potential applications. Prog Mater Sci 97:230-282. https://doi.org/10.1016/j.pmatsci.2018.05.001
5. Dolmaire N, Méchin F, Espuche É (2006) Water transport in polyurethane/polydimethylsiloxane membranes: Influence of the hydrophobic/hydrophilic balance and of the crosslink density. Desalination 199(1-3):118-120. https://doi.org/10.1016/j.desal.2006.03.154
6. Wypych G (2022) Handbook of polymers. Elsevier, Canada, pp 579-584, pp 665-668
7. Drobny JG (2014) Handbook of thermoplastic elastomers. Elsevier, New Jersey, pp 9-16, pp 215-221
8. Mansouri M, Ghadimi A, Gharibi R, Norouzbahari S (2021) Gas permeation properties of highly cross-linked castor oil-based polyurethane membranes synthesized through thiol-yne click polymerization. React Funct Polym 158:104799. https://doi.org/10.1016/j.reactfunctpolym.2020.104799
9. Maher BM, Rezaali J, Ghaleh H et al (2017) Evaluation of poly (2-hydroxyethyl methacrylate) and poly (methyl methacrylate)-grafted poly (vinylidene fluoride)-poly (dimethyl siloxane) bilayers for gas separation. Colloid Polym Sci 295(9):1595–1607. https://doi.org/10.1007/s00396-017-4124-7
10. Eusébio TM, Martins AR, Pon G et al (2020) Sorption/Diffusion contributions to the gas permeation properties of bi-soft segment polyurethane/polycaprolactone membranes for membrane blood oxygenators. Membranes 10(1):8. https://doi.org/10.3390/membranes10010008
11. Low SC, Murugaiyan SV (2021) Thermoplastic Polymers in Membrane Separation. https://doi:10.1016/B978-0-12-820352-1.00083-3
12. Melnig V, Apostu MO, Tura V, Ciobanu C (2005) Optimization of polyurethane membranes: Morphology and structure studies. J Membr Sci 267(1-2):58-67. https://doi.org/10.1016/j.memsci.2005.04.054

13. Shahzamani M, Ebrahimi NG, Sadeghi M, Mostafavi F (2016) Relationship between the Microstructure and Gas Transport Properties of Polyurethane/Polycaprolactone Blends. IJChE 13(3):78-88
14. Baker RW (2004) Membrane technology and applications. John Wiley & Sons, California, pp 9-16, pp 215-221
15. Wolińska-Grabczyk A (2006) Effect of the hard segment domains on the permeation and separation ability of the polyurethane-based membranes in benzene/cyclohexane separation by pervaporation. J Membr Sci 282(1-2):225-236. https://doi.org/10.1016/j.memsci.2006.05.026
16. Semsarzadeh MA, Sadeghi M, Barikani M (2007) The effect of hard segments on the gas separation properties of polyurethane membranes. Iran Polym J 16(12):819-827
17. Shahzamani M, Ebrahimi NG, Sadeghi M, Mostafavi F (2016) Relationship between the Microstructure and Gas Transport Properties of Polyurethane/Polycaprolactone Blends. IJChE 13(3):78-88
18. Szycher M (2013) Polyurethanes. Taylor & Francis Group CRC Press, New York, pp 1-6, pp 41-50
19. Fakhar A, Sadeghi M, Dinari M, Lammertink R (2019) Association of hard segments in gas separation through polyurethane membranes with aromatic bulky chain extenders. J Membr Sci 574:136-146. https://doi.org/10.1016/j.memsci.2018.12.062
20. Sadeghi M, Talakesh MM, Arabi Shamsabadi A, Soroush M (2018) Novel application of a polyurethane membrane for efficient separation of hydrogen sulfide from binary and ternary gas mixtures. ChemistrySelect 3(11):3302-3308. https://doi.org/10.1002/slct.201703170
21. Santos GH, Rodrigues MA, Ferraz HC, Moura LC, de Miranda JL (2019) A More Sustainable Polyurethane Membrane for Gas Separation at Room Temperature and Low Pressure. In Materials Science Forum 965:125-132. https://doi.org/10.4028/www.scientific.net/MSF.965.125
22. Fakhar A, Sadeghi M, Dinari M et al (2020) Elucidating the effect of chain extenders substituted by aliphatic side chains on morphology and gas separation of polyurethanes. Eur Polym J 122:109346. https://doi.org/10.1016/j.eurpolymj.2019.109346
23. Norouzbahari S, Gharibi R (2020) An investigation on structural and gas transport properties of modified cross-linked PEG-PU membranes for CO_2 separation. React Funct Polym 151:104585. https://doi.org/10.1016/j.reactfunctpolym.2020.104585
24. Turan D, Sängerlaub S, Stramm C, Gunes G (2017) Gas permeabilities of polyurethane films for fresh produce packaging: response of O_2 permeability to temperature and relative humidity. Polym Test 59:237-244. https://doi.org/10.1016/j.polymertesting.2017.02.007
25. Isfahani AP, Sadeghi M, Wakimoto K et al (2017) Enhancement of CO_2 capture by polyethylene glycol-based polyurethane membranes. J Membr Sci 542:143-149. https://doi.org/10.1016/j.memsci.2017.08.006
26. Adam NI, Hanibah H, Subban RHY et al (2020) Palm-based cationic polyurethane membranes for solid polymer electrolytes application: A physico-chemical characteristics studies of chain-extended

cationic polyurethane. Ind Crop Prod 155:112757. https://doi.org/10.1016/j.indcrop.2020.112757

27. Sadeghi M, Semsarzadeh MA, Barikani M, Ghalei B (2011) Study on the morphology and gas permeation property of polyurethane membranes. J. Membr. Sci. 385:76-85. https://doi.org/10.1016/j.memsci.2011.09.024
28. Liu L, Huang ZM, He CL, Han XJ (2006) Mechanical performance of laminated composites incorporated with nanofibrous membranes. Mater Sci Eng 435:309-317. https://doi.org/10.1016/j.msea.2006.07.064
29. Eusébio TM, Faria M, Filipe EJ, de Pinho MN (2019) Polyurethane urea membranes for membrane blood oxygenators: Synthesis and gas permeation properties. ENBENG 1-4 IEEE
30. Babaie A, Rezaei M, Sofla RLM (2019) Investigation of the effects of polycaprolactone molecular weight and graphene content on crystallinity, mechanical properties and shape memory behavior of polyurethane/graphene nanocomposites. J mech behav of biomed 96:53-68. https://doi.org/10.1016/j.jmbbm.2019.04.034
31. Storey RF, Sherman JW (2002) Kinetics and mechanism of the stannous octoate-catalyzed bulk polymerization of ε-caprolactone. Macromolecules 35(5):1504-1512. https://doi.org/10.1021/ma010986c
32. Lipik VT, Abadie MJ (2010) Process optimization of poly (ε-caprolactone) synthesis by ring-opening polymerization. Iran Polym J 19(11):885-893
33. Crescenzi V, Manzini G, Calzolari G, Borri C (1972) Thermodynamics of fusion of poly-β-propiolactone and poly-ϵ-caprolactone. comparative analysis of the melting of aliphatic polylactone and polyester chains. Eur Polym J 8(3):449-463. https://doi.org/10.1016/0014-3057(72)90109-7
34. Eyvazzadeh Kalajahi A, Rezaei M, Abbasi F (2016) Preparation, characterization, and thermomechanical properties of poly (ε-caprolactone)-piperazine-based polyurethane-urea shape memory polymers. Mater Sci 51(9):4379-4389 https://doi.org/10.1007/s10853-016-9750-9
35. Eyvazzadeh Kalajahi A, Rezaei M, Abbasi F, Mir Mohamad Sadeghi G (2017) The effect of chain extender type on the physical, mechanical, and shape memory properties of poly (ε-caprolactone)-based polyurethane-ureas. Polym Plast Tech Eng 56(18):1977-1985. https://doi.org/10.1080/03602559.2017.1298797

Figures

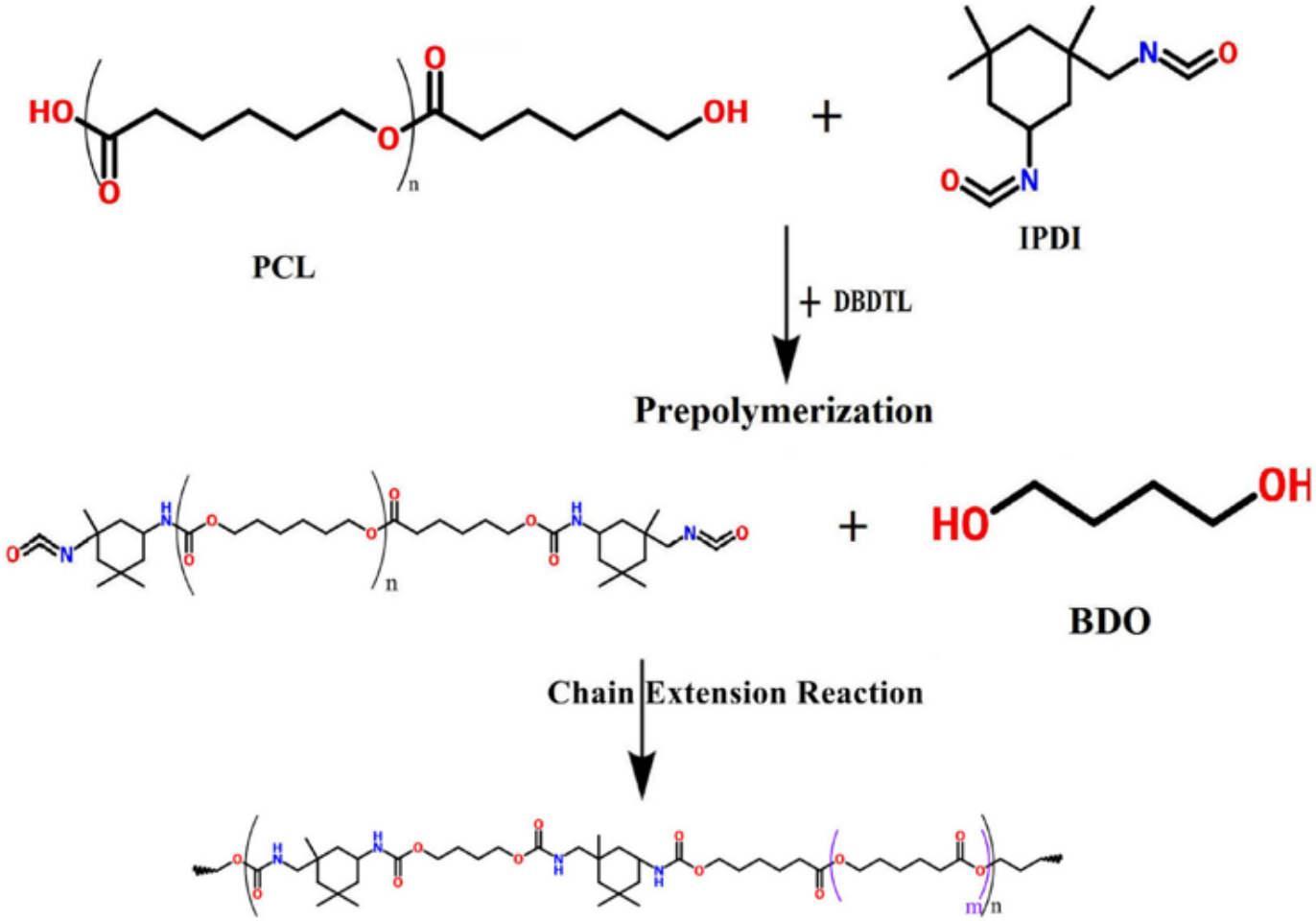

Figure 1

Schematic synthesis route for the preparation of TPU.

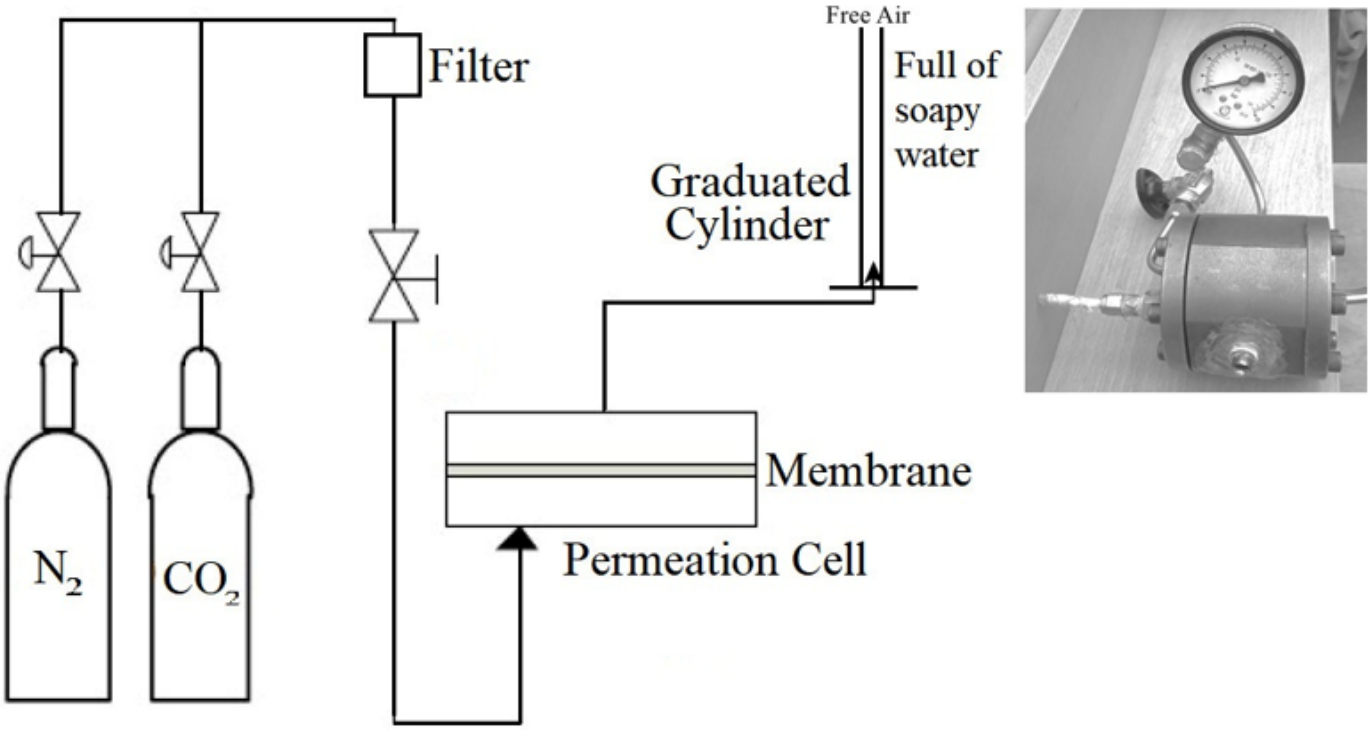

Figure 2

Schematic view of gas permeation device

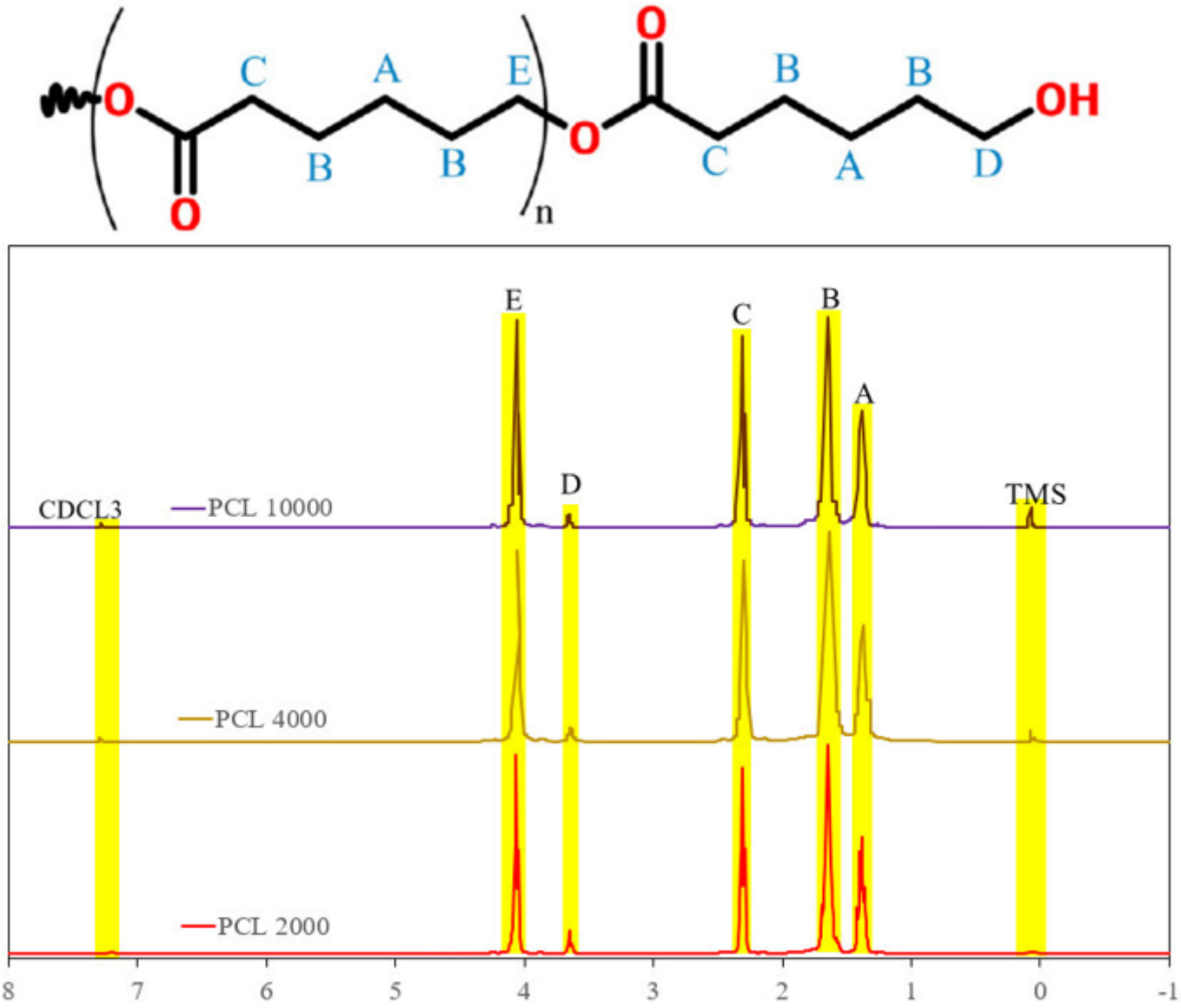

Figure 3

H-NMR spectra of synthesized PCLs with various molecular weights.

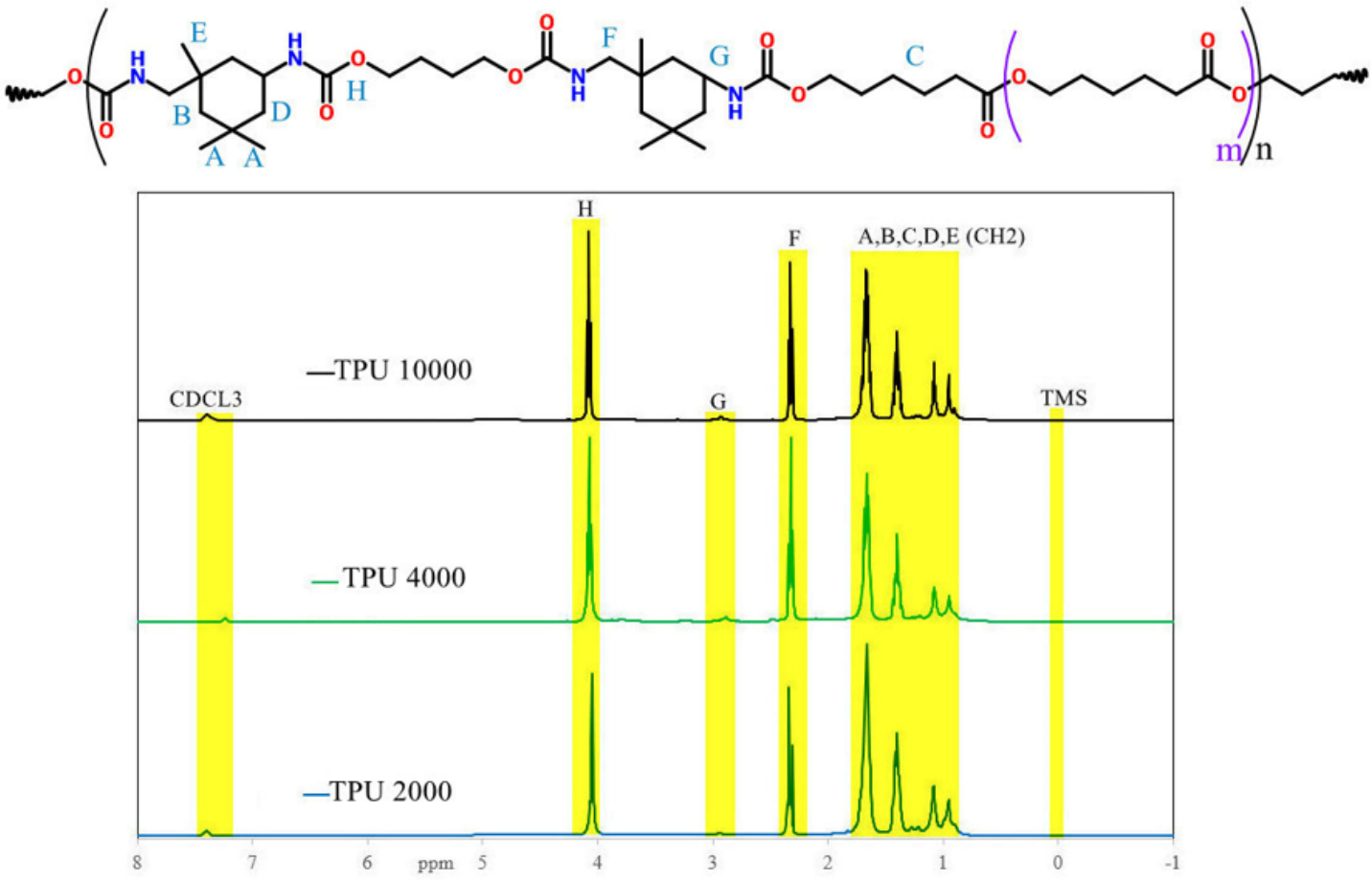

Figure 4

H-NMR spectra of synthesized TPUs.

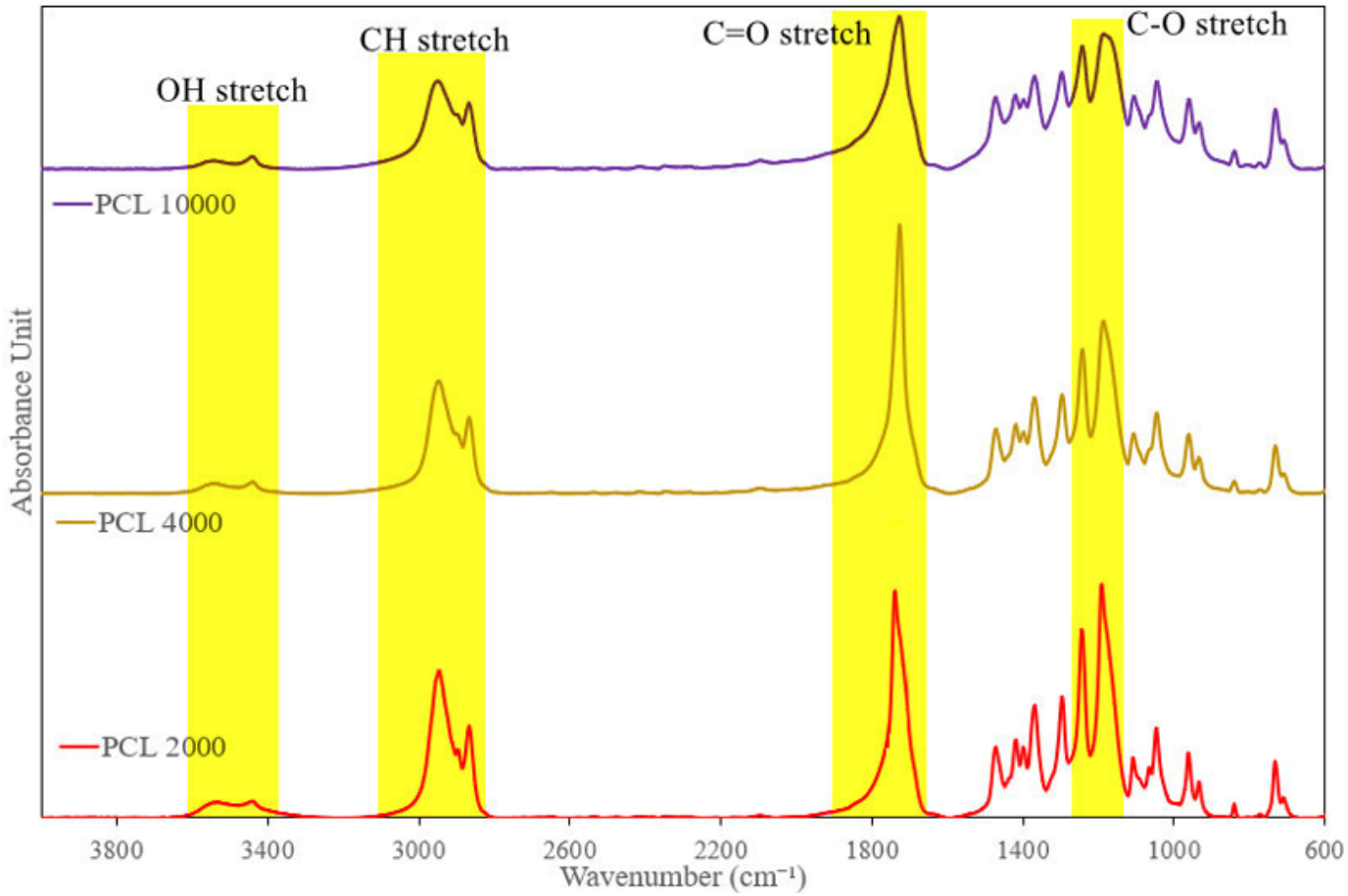

Figure 5

FTIR spectra of synthesized PCLs.

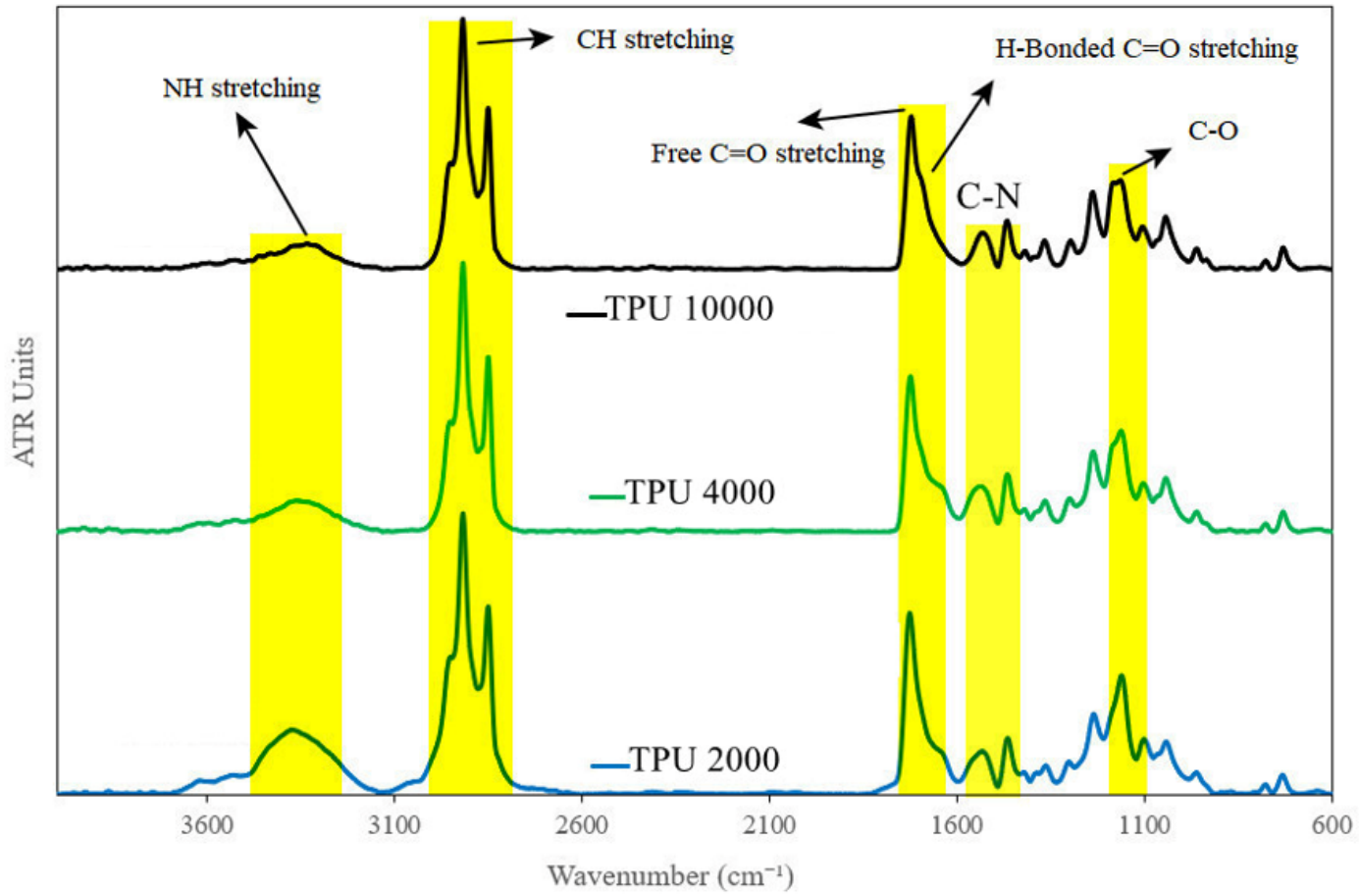

Figure 6

FTIR spectra of synthesized TPUs.

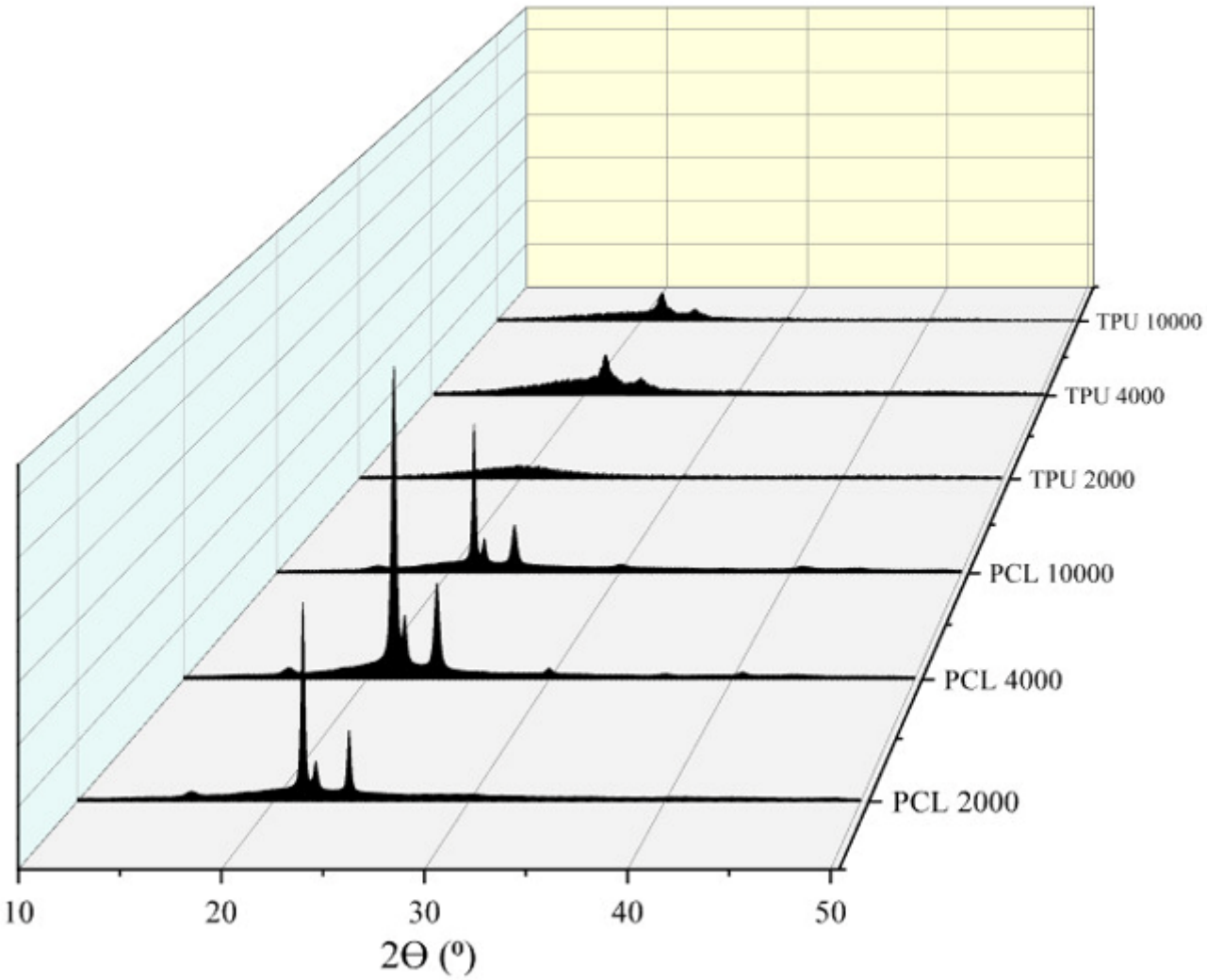

Figure 7

XRD patterns of synthesized PCL & TPU samples.

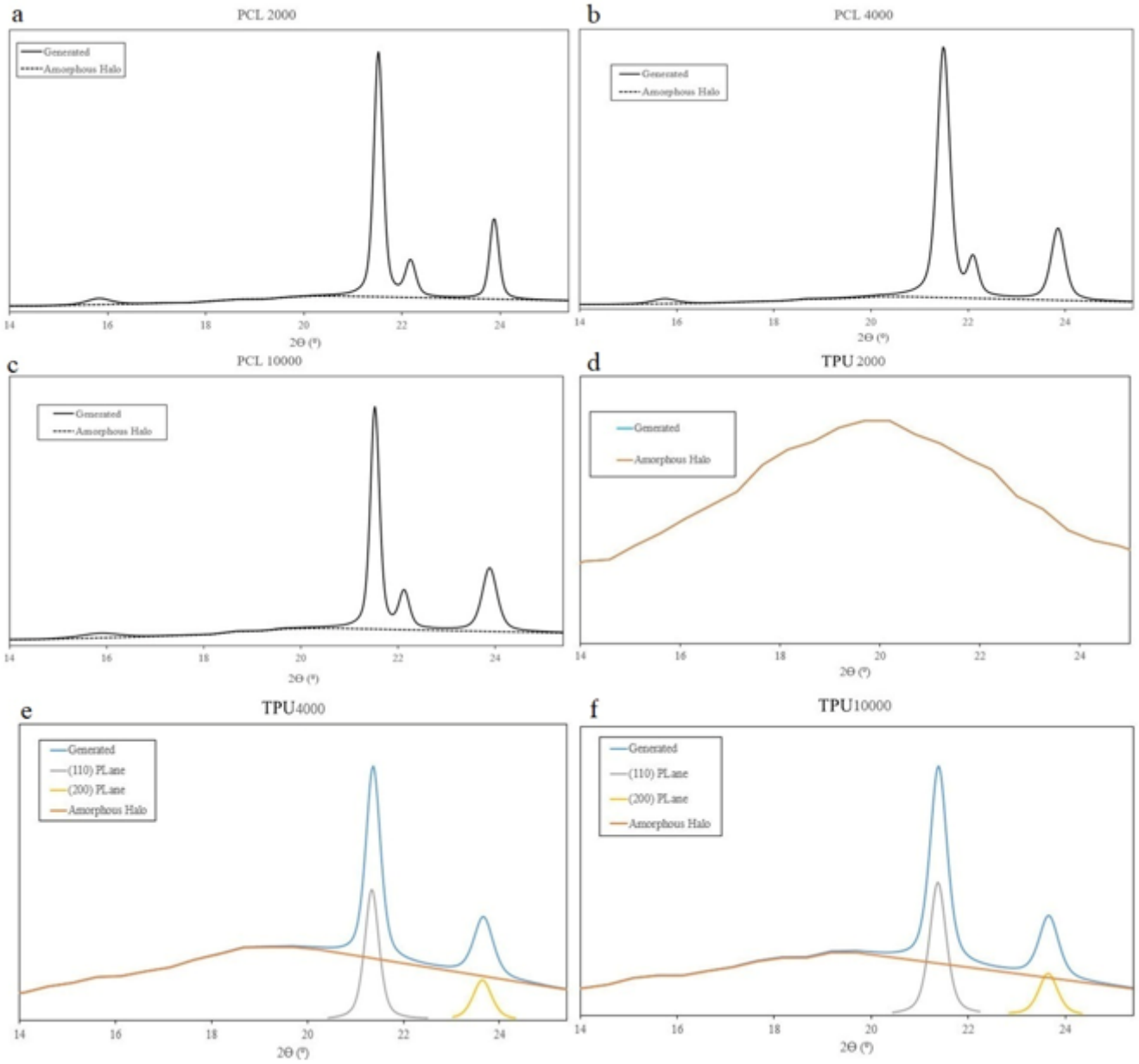

Figure 8

XRD patterns of all samples, crystals with (110), (200) orientations, and amorphous halo of different samples.

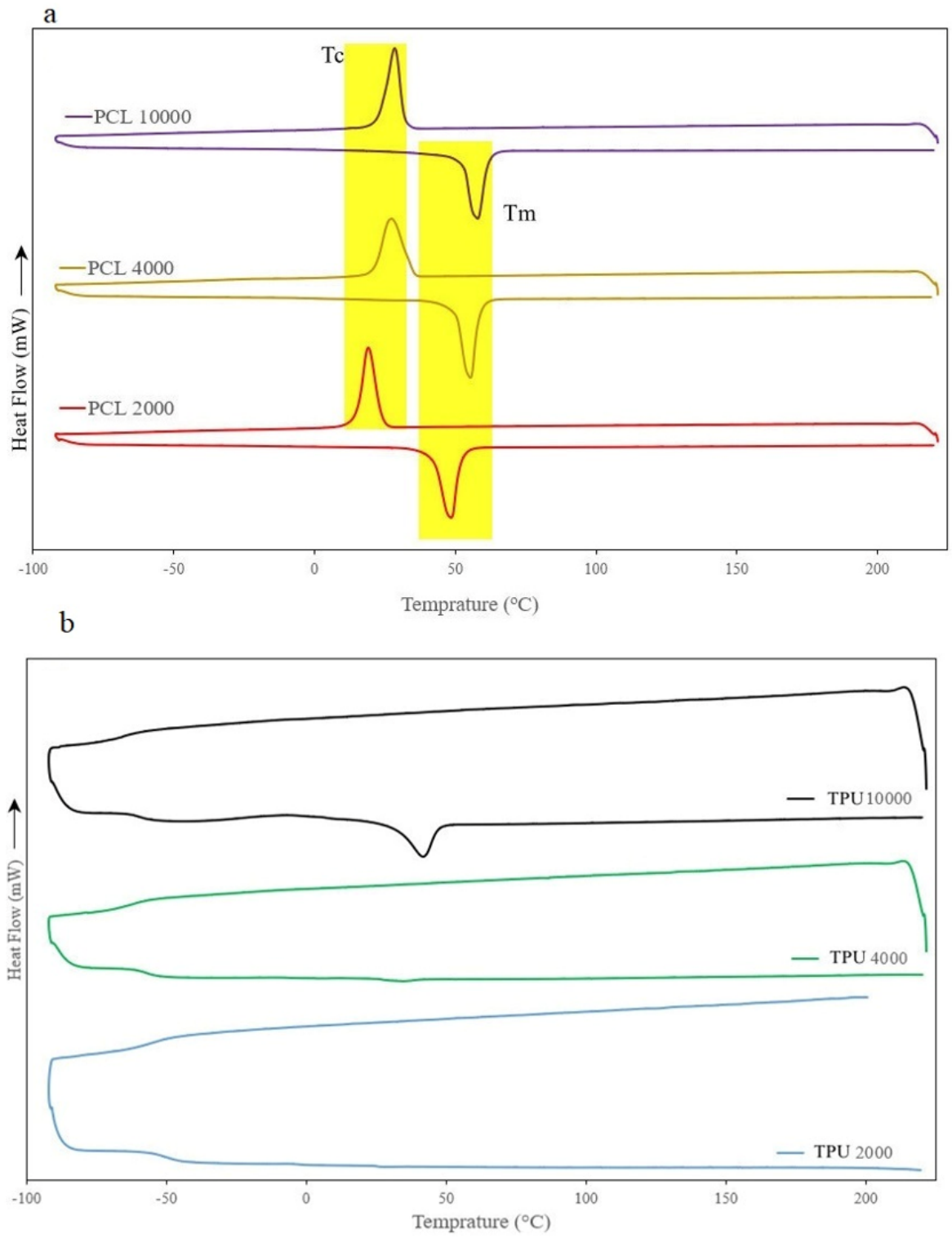

Figure 9

The DSC thermograms of synthesized PCLs (a) & TPUs (b).

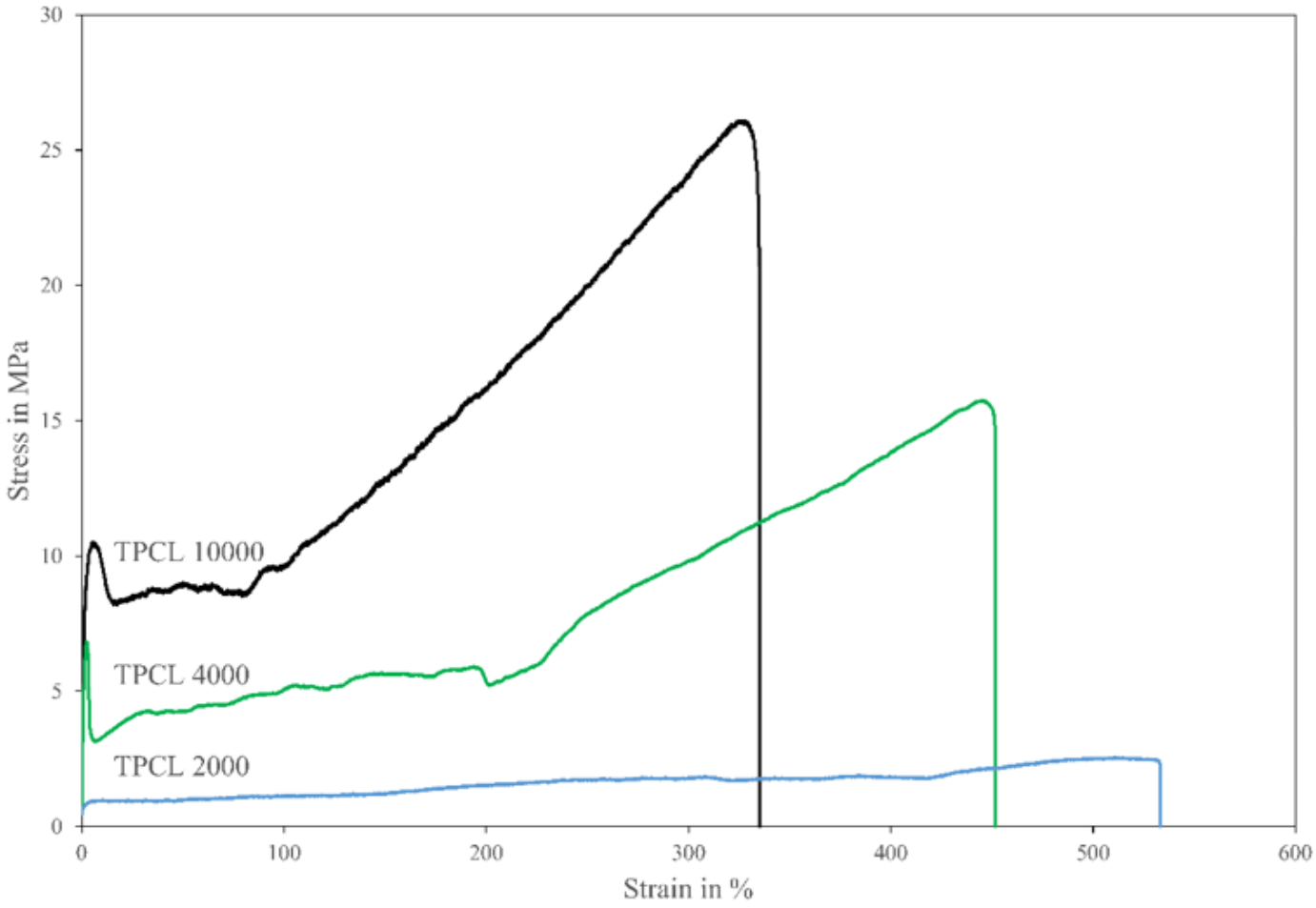

Figure 10

Tensile stress-strain curves of prepared TPU membranes

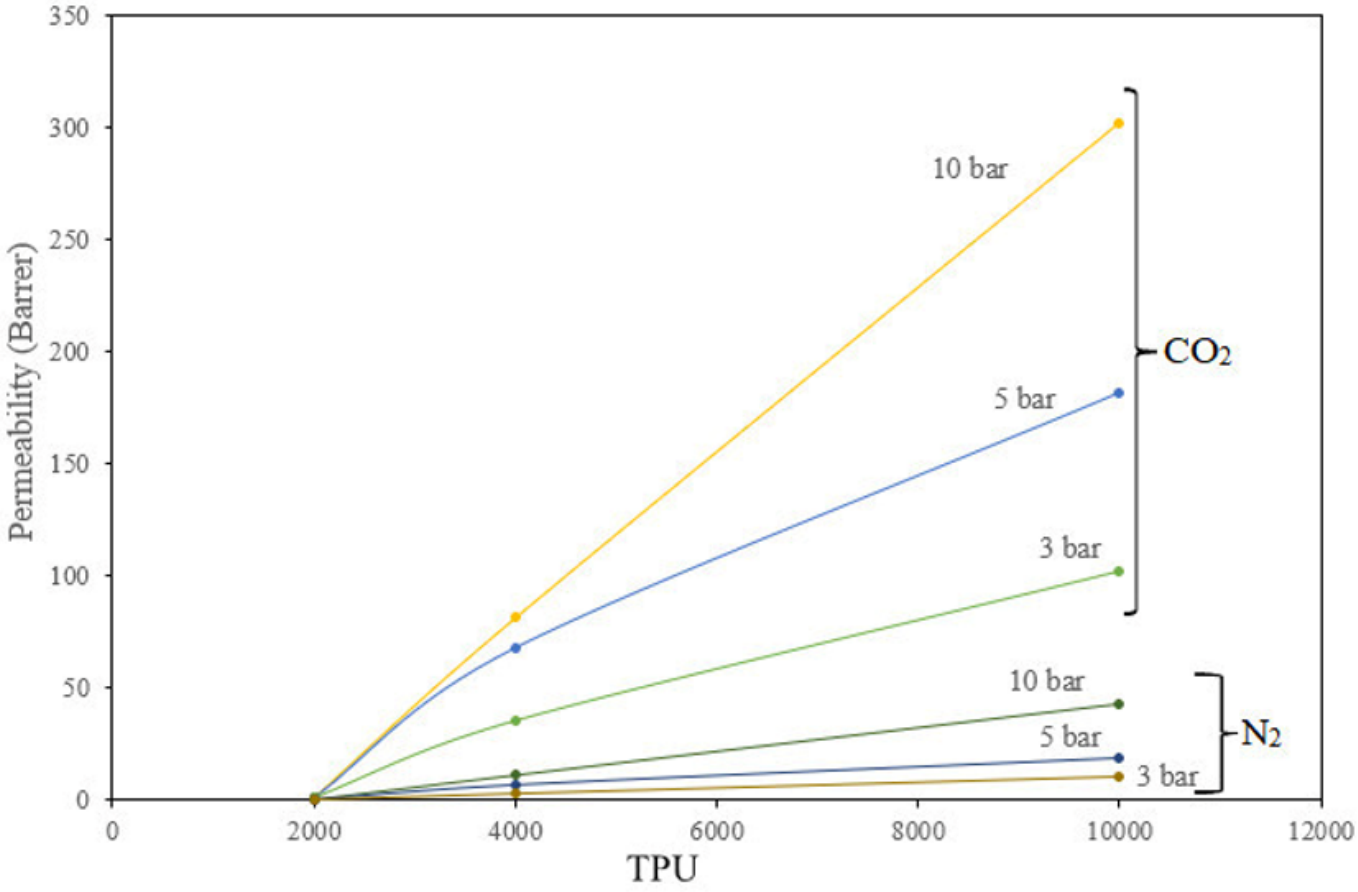

Figure 11

Variation of permeability in TPU membranes with pressure for CO_2 and N_2 gases. The lines are used to guide the eyes